

# LHC Bounds on Interactions of Dark Matter

Arvind Rajaraman, William Shepherd, Tim M.P. Tait and Alexander M. Wijangco

*Department of Physics and Astronomy,  
University of California, Irvine, California 92697*

(Dated: August 8, 2011)

## Abstract

We derive limits on the interactions of dark matter with quarks from ATLAS null searches for jets + missing energy based on  $\sim 1 \text{ fb}^{-1}$  of integrated luminosity, using a model-insensitive effective theory framework. We find that the new limits from the LHC significantly extend limits previously derived from CDF data at the Tevatron. Translated into the parameter space of direct searches, these limits are particularly effective for  $\sim \text{GeV}$  mass WIMPs. Our limits indicate tension with isospin violating models satisfying minimal flavor violation which attempt to reconcile the purported CoGeNT excess with Xenon-100, indicating that either a light mediator or nontrivial flavor structure for the dark sector is necessary for a viable reconciliation of CoGeNT with Xenon.

arXiv:1108.1196v1 [hep-ph] 4 Aug 2011

## I. INTRODUCTION

The evidence for the existence of dark matter in the universe is overwhelming [1], and models to incorporate dark matter into our understanding of the fundamental physics of the universe are myriad. Astrophysical observations tell us nothing about the mass of the dark matter particle or whether it interacts with the Standard Model (SM) particles in any way other than gravitationally. Models range in masses from keV to the GUT scale, and in coupling strength from slightly weaker than QCD couplings to purely gravitational interactions. The most popular models are driven by the WIMP(less) miracle [2], suggesting that the dark matter particle relic density should naturally be set by the thermal history of the universe and favoring a ratio of the mass and coupling strength. Such dark matter candidates naturally appear in extensions of the Standard Model which are designed to address other theoretical issues, most notably the gauge hierarchy problem. Since WIMPs have fairly large couplings to SM fields to explain their relic density, it is possible to search for them interacting directly with normal matter, annihilating into normal matter, or being produced at high energy colliders.

Any WIMP which produces a signal in one of these searches would naively be expected to be seen in others as well, as a single coupling could be visible to all of them. Each type of experiments has a particular set of strengths and weaknesses associated with its ability to discover or exclude various models of dark matter. Direct detection experiments have a signal that is strongly peaked at very low energies, making it hard to distinguish from background effects and causing detector thresholds to be particularly troublesome when light candidate particles are considered. Indirect detection searches for dark matter annihilation products are able to observe locations which have much higher local densities of dark matter than our solar system, but then must contend with large astrophysical background uncertainties. Colliders have a fixed amount of energy available to them in the collisions (and do not take advantage of the dark matter already present in the galactic halo), and are thus unable to produce dark matter of very large mass, but have exceptional sensitivity to low mass WIMPs, which are ill constrained by the other two techniques. Any signal seen at colliders may be due to other new physics than dark matter, so astrophysical confirmation will be critical to being able to make robust claims regarding dark matter at colliders. However, colliders are able to make strong exclusion statements in the event of no signal [3–17].

Currently there is much interest in light WIMP models, with masses of order  $\lesssim 10$  GeV, motivated in large part by experimental results from the CoGeNT collaboration [18, 19] which can be explained by such a WIMP and appear to be tantalizingly close to the parameter space favored by a dark matter interpretation of the longstanding DAMA annual modulation signal [20–22]. As the CoGeNT collaboration has recently reported that they also see annual modulation in their data [19], these results have only grown more interesting. These putative signals are, however, in significant tension with negative results from the Xenon 100 [23] and CDMS-II [24–26] collaborations, and the modulation exhibits an unexpected dependence on the recoil energy of the scattered nucleus [27–29].

In this work we extend previous studies [8–11, 30] which use the framework of effective field theory to construct models of dark matter and constrain them from collider searches. These models make specific predictions for other dark matter searches as well, and allow the collider constraints to be drawn on a direct detection plane. Similarly, constraints from indirect searches can be interpreted in these models on the plane of direct detection [31–33]. We enlarge our previous set of effective theories to allow couplings to only one type of quarks at a time. This allows for the inclusion of effects which distinguish between quark charge in the model-independent framework which we previously presented and are more representative of the range of possible couplings present in models with minimal flavor violation (MFV) [34]. In particular, the dependence on  $\tan \beta$  expected in type-II two Higgs doublet extensions of the SM (such as in the Minimal Supersymmetric Standard Model) can be easily represented in this set of models, in contrast to our previous work.

A recent proposal [35, 36] suggests that dark matter interactions may be sensitive to the specific proton and neutron content of the nucleus with which it is scattering, rather than just the net baryon number (the mass of the nucleus). For a WIMP whose couplings satisfy  $\lambda_n/\lambda_p \sim -0.7$ , one obtains consistency between the negative results of the Xenon collaboration and the putative signal seen at CoGeNT by largely canceling the coupling to xenon nuclei. This parameter point has the additional feature that it shifts the DAMA target region such that it moves from being close to but inconsistent with the CoGeNT signal, to a situation where CoGeNT and DAMA are fit by consistent choices of parameters. In a short time, many models predicting or utilizing this “isospin-violating” mechanism have appeared in the literature [37–41].

This article is organized as follows: In section II we discuss the effective field theory mod-

eling of WIMP-SM interactions, in section III we calculate bounds on the strength of dark matter interactions using collider data and present future reach for the LHC, in section IV we discuss the impact of these bounds on direct detection signals, and in section V we present our conclusions.

## II. MODEL DESCRIPTION

In formulating our constraints on dark matter from collider searches we assume that the dark matter candidate is the only new particle which is accessible at the relevant experiments and that dark matter is a SM gauge singlet. Under these assumptions, only non-renormalizable couplings are possible between dark matter and the SM fields. We therefore focus on the operators which are of the lowest dimensionality, as these will give the strongest signals at energies below the scale which characterizes the interactions.

As with any effective field theory, the models of dark matter we construct in this way are only applicable below some cutoff scale where other new physics becomes relevant and renormalizability is regained. This cutoff is approximately at the mass of the lowest-lying state which is integrated out in the effective theory. This is related to the scale suppressing the higher-dimensional operators and the couplings of the fundamental theory as

$$M_* \sim \frac{M_\Phi}{g_\Phi}, \quad (1)$$

where  $\Phi$  is the field which has been integrated out to give the interaction whose strength is parametrized by  $M_*$ . Note that this relation tells us that below a certain value of  $M_*$  it is not possible to have a perturbative completion of the theory involving exchange of particles whose masses are all larger than the WIMP mass; we discard results in such regions as it is clear there is no perturbative UV completion of the effective theory in this regime [8].

In this work our primary focus is on the effect that isospin violation can have on collider constraints on dark matter, so we will specialize to the case of a Majorana WIMP, as constraints on the isospin violating couplings from colliders are not expected to depend sensitively on the nature of the dark matter candidate [8–10]. As we are particularly interested in relating to direct detection, we focus on couplings of dark matter to quarks. Gluon couplings are also interesting for direct detection, but they are not able to differentiate between states of different isospin. We therefore do not consider couplings of dark matter to gluons

Name	$G_\chi$	$\Gamma_\chi$	$\Gamma_q$
M1	$m_q/2M_*^3$	1	1
M2	$im_q/2M_*^3$	$\gamma_5$	1
M3	$im_q/2M_*^3$	1	$\gamma_5$
M4	$m_q/2M_*^3$	$\gamma_5$	$\gamma_5$
M5	$1/2M_*^2$	$\gamma_5\gamma_\mu$	$\gamma^\mu$
M6	$1/2M_*^2$	$\gamma_5\gamma_\mu$	$\gamma_5\gamma^\mu$

TABLE I: The list of the effective operators defined in Eq. (2).

in this work.

We construct all of the lowest-dimension operators that couple dark matter and quarks consistent with MFV, which helps ensure that the models which we produce are not in conflict with flavor physics observables [13]. This amounts to the assumption that any term which breaks  $SU(2)_L$  of the SM must do so through the SM Yukawa couplings, leading to the suppression by the quark mass of any operator which flips the quark chirality. The leading operators are of the form

$$L_{Eff} = G_\chi \bar{\chi}\Gamma_\chi\chi \bar{q}\Gamma_qq \quad (2)$$

where

$$\Gamma_{\chi,q} \in \{1, \gamma^5, \gamma^\mu, \gamma^\mu\gamma^5, \sigma^{\mu\nu}\}. \quad (3)$$

Any other combination of bilinears are equivalent to a linear combination of this set through Fierz identities. Note that any Lorentz indices in  $\Gamma_\chi$  must be contracted with indices in  $\Gamma_q$  to preserve Lorentz invariance. Thus our models contain no tensor terms, because it vanishes for Majorana particles and the alternatives are higher order in derivatives, and thus more suppressed in low energy reactions. The MFV assumption requires us to scale quark bilinears with no Lorentz indices by the quark mass, and to have no relative scaling between the couplings for different quarks in bilinears carrying a Lorentz index. However, we still have two independent coefficients for each operator structure associated with up- and down-type quark couplings, which are not constrained relative to each other by MFV.

The list of all operator Lorentz structures we consider are presented in Table I. Note that the cases of up- and down-type couplings are distinguished in our notation by a trailing u

or d on the designator of the Lorentz structure. For example, operator M1u corresponds to

$$\mathcal{L}_{\text{M1u}} = \frac{1}{2M_*^3} \bar{\chi}\chi \sum_{q=u,c,t} m_q \bar{q}q. \quad (4)$$

### III. COLLIDER SEARCHES

We constrain the operators by simulating the production of a pair of WIMPs and jets at colliders,

$$pp(p\bar{p}) \rightarrow \chi\chi + \text{jets} \quad (5)$$

As the WIMPs are invisible to the particle detectors, such a process would appear as a combinations of jets and missing energy. We estimate efficiencies for the signal to pass analysis cuts (outlined below) based on simulations using Madgraph 4.5.0, with showering and detector simulation performed by the Madgraph Pythia-PGS 2.8 package [42–44]. The dominant standard model background for such a signal is  $Z + \text{jets}$ , where the  $Z$  boson then decays to a pair of neutrinos. The next largest background is  $W + \text{jets}$ , where the  $W$  decays into a neutrino and a charged lepton which is mistagged to be a jet or lost [45–47].

We assume only one Lorentz structure is dominant at a time, and constrain each by assuming the others do not contribute to the cross section. Since the coupling of models with scalar Lorentz structures are proportional to quark mass, the cross sections from down-type operators are enhanced by the bottom quark mass (though moderated by the  $b$  parton distribution function), resulting in stronger bounds on operators M1d–M4d compared to M1u–M4u. For models with vector Lorentz structure, the parton distribution functions are the dominant difference between the up-type and down-type operators, resulting in comparatively stronger constraints upon the up-type couplings.

#### A. Tevatron Constraints

The CDF collaboration has reported null results for a mono-jet search based on about 1 fb<sup>-1</sup> of Tevatron run II data [46], constraining the size of additional contributions to missing energy + jets. The analysis selects events which have missing transverse momentum  $\cancel{E}_T > 80$  GeV together with a leading jet whose transverse momentum is  $p_T > 80$  GeV. A second jet with  $p_T < 30$  GeV is allowed, and any subsequent jets must have  $p_T < 20$  GeV. In a

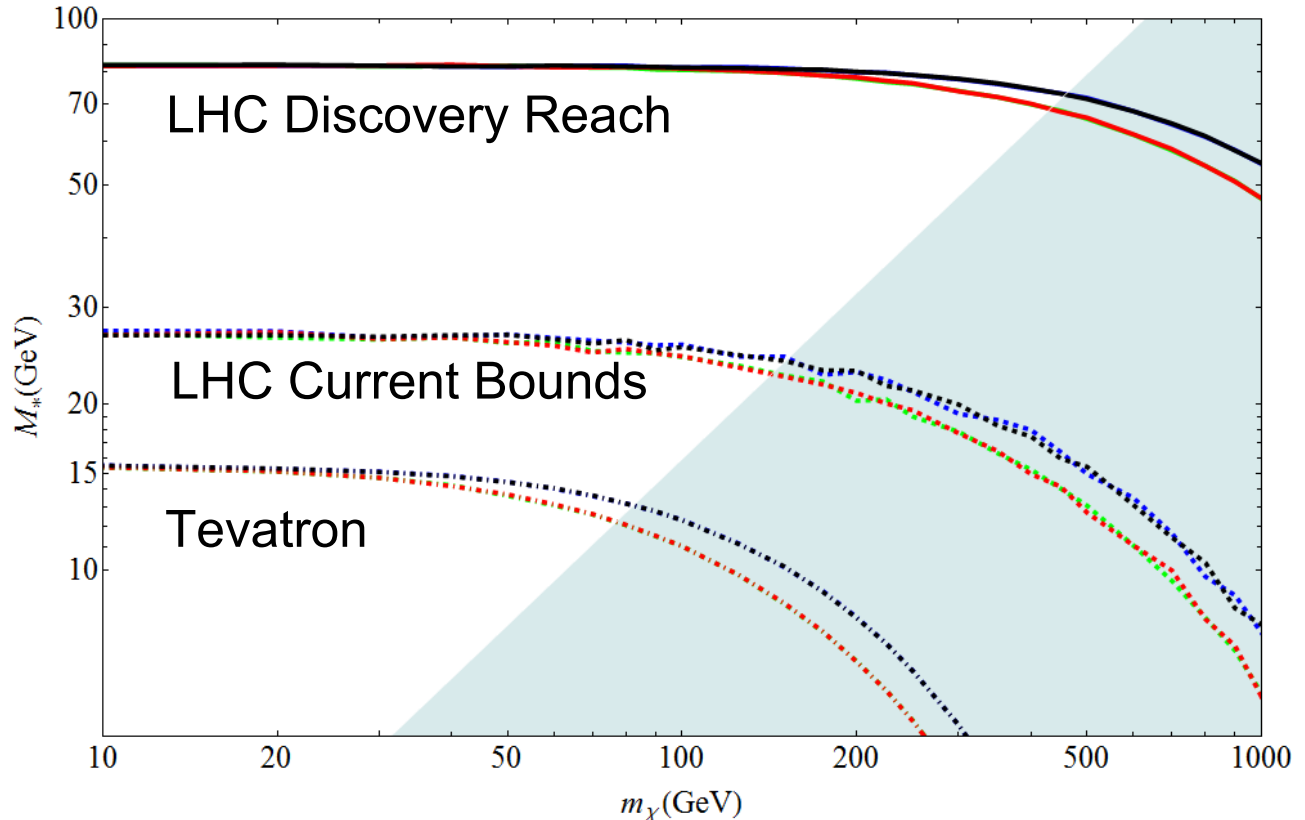


FIG. 1: The collider bounds on the down-type quark operators with scalar Lorentz structures. Operators M1d, M2d, M3d, M4d, are in red, blue, green, and black respectively. The dashed-dotted, dashed, and solid lines are the Tevatron constraints, LHC constraints, and LHC discovery reach. The shaded region is where the effective theory breaks down. Models M1d and M3d are largely degenerate, as are models M2d and M4d.

sample size of  $1 \text{ fb}^{-1}$ , CDF found 8449 events while the Standard Model prediction was  $8663 \pm 332$  events. To be within  $2\sigma$  of these results, the accepted cross section of new physics can be at most  $0.664 \text{ pb}$ . In Figures 1 - 4, we translate the cross section limit into one on  $M_*$  for each operator, as a function of the dark matter mass.

## B. LHC Constraints

The ATLAS Collaboration has very recently released the results of a search for anomalous production of jets and missing energy at  $\sqrt{s} = 7 \text{ TeV}$  with an integrated luminosity of  $1.00 \text{ fb}^{-1}$  [47]. Events with  $\cancel{E}_T > 120 \text{ GeV}$  and containing a leading jet with  $p_T > 120 \text{ GeV}$

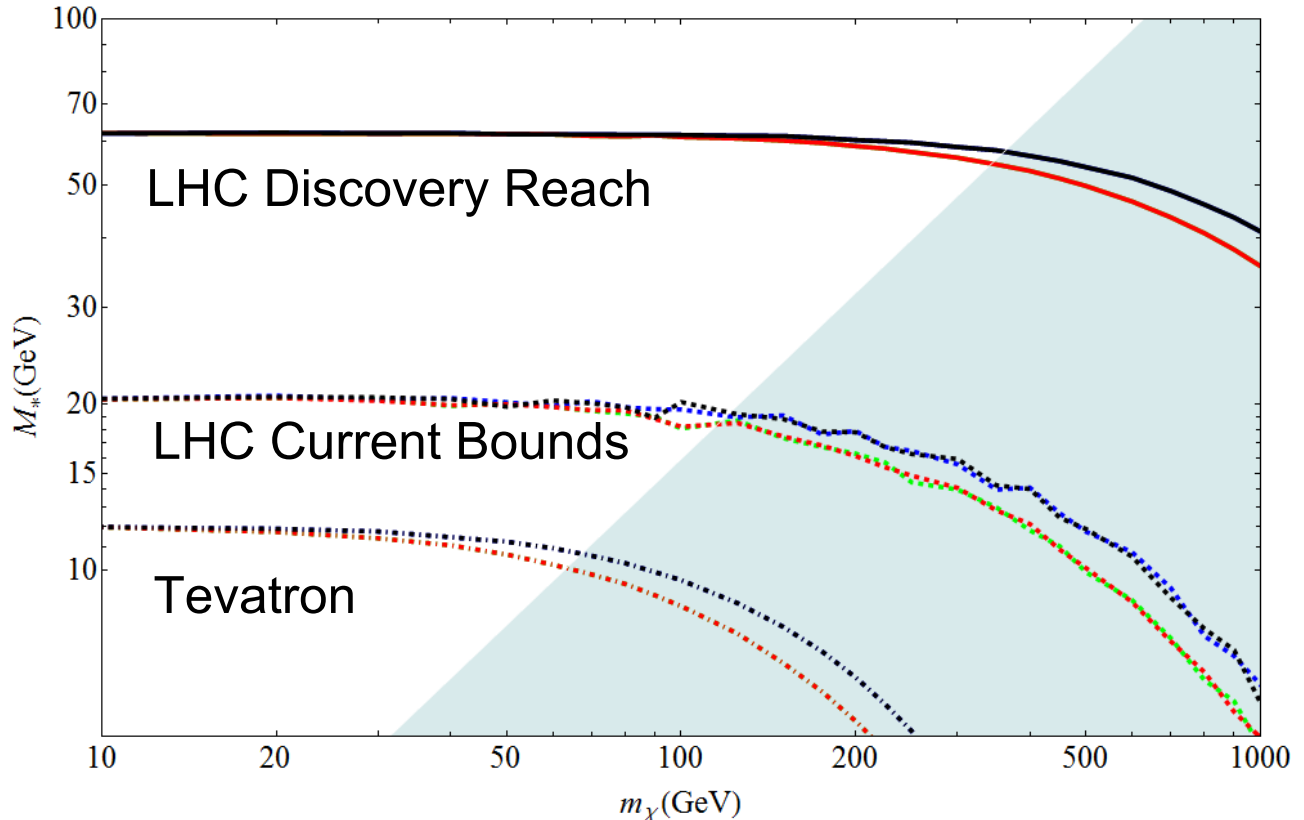


FIG. 2: The same as Fig. 1, for up-type quark operators M1u, M2u, M3u, and M4u.

and  $|\eta| < 2$  were selected. A second jet with  $p_T < 30$  GeV and  $|\eta| < 4.5$  was allowed. 15740 events were observed, to be compared with an expected  $15100 \pm 170(\text{stat.}) \pm 680(\text{syst.})$ . This excludes an effective cross section of 1.7 pb, which we map to constraints upon  $M_*$  in Figures 1 - 4.

### C. LHC Future Reach

We also investigate the  $5\sigma$  discovery reach of such operators, using the analysis done in [48], which considered the LHC running at  $\sqrt{s} = 14$  TeV and with an integrated luminosity of  $100 \text{ fb}^{-1}$ . Events with missing  $\cancel{E}_T > 500$  GeV and at least one a jet with  $p_T > 500$  GeV were considered, but no secondary jet rejection cut was employed. Events with isolated charged leptons were rejected. Ref [48] predicts a Standard Model background of about  $B = 3 \times 10^4$  events for this integrated luminosity. We determine the discovery reach by requiring that the significance of the new physics signal  $S$  passing the cuts satisfy  $S/\sqrt{B} \geq 5$  and plot the

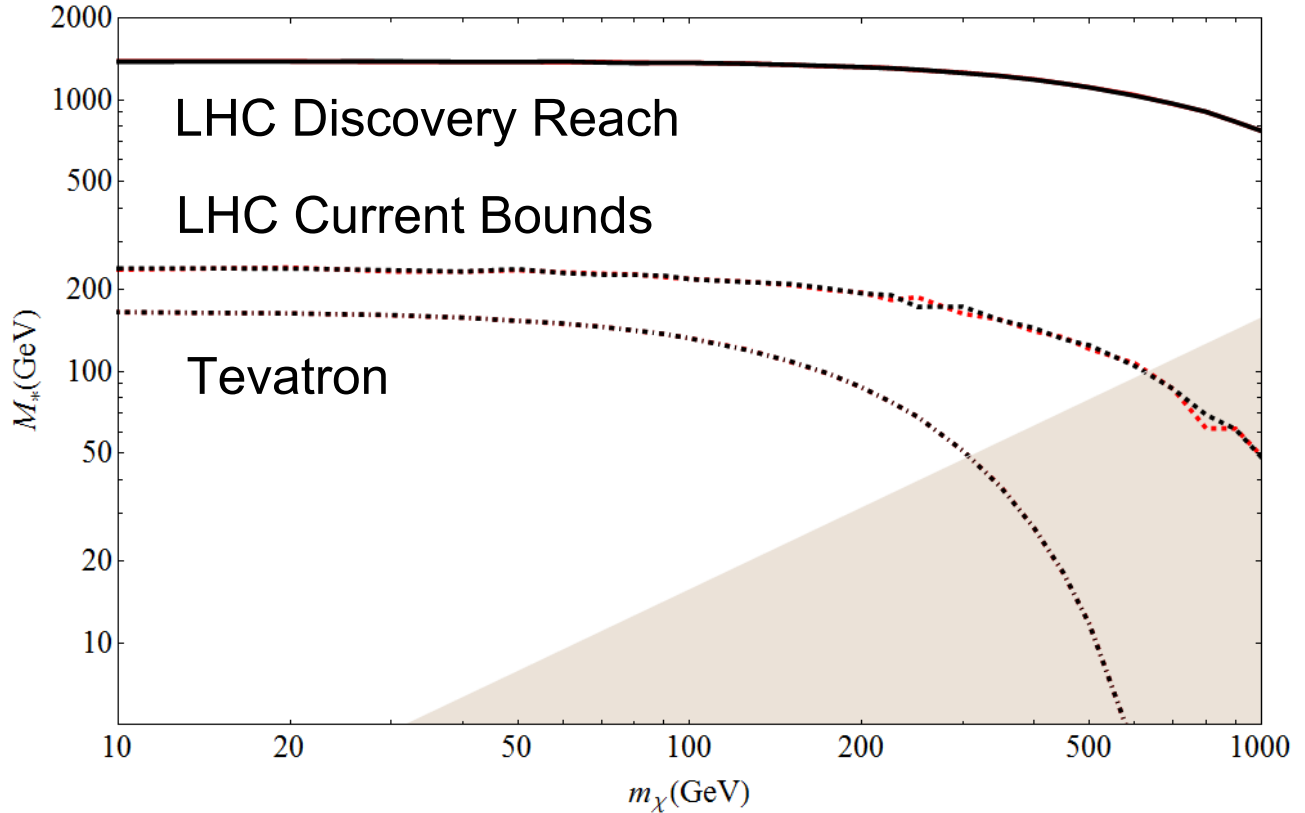


FIG. 3: The collider bounds on the down-type quark coupling operators mediated by a heavy scalar. Models M5d, M6d are in red, black respectively. The dashed-dotted, dashed, and solid lines are the Tevatron constraints, LHC constraints, and LHC discovery reach. The shaded region is where the effective theory breaks down. Models M5d and M6d are largely degenerate.

resulting region in Figures 1 - 4.

#### IV. DIRECT DETECTION

Our effective theory allows one to translate the collider bounds into the parameter space of direct detection experiments. In the non-relativistic limit, only operators M1d, M1u, M6d, and M6u mediate unsuppressed scattering cross sections with nucleons. In terms of

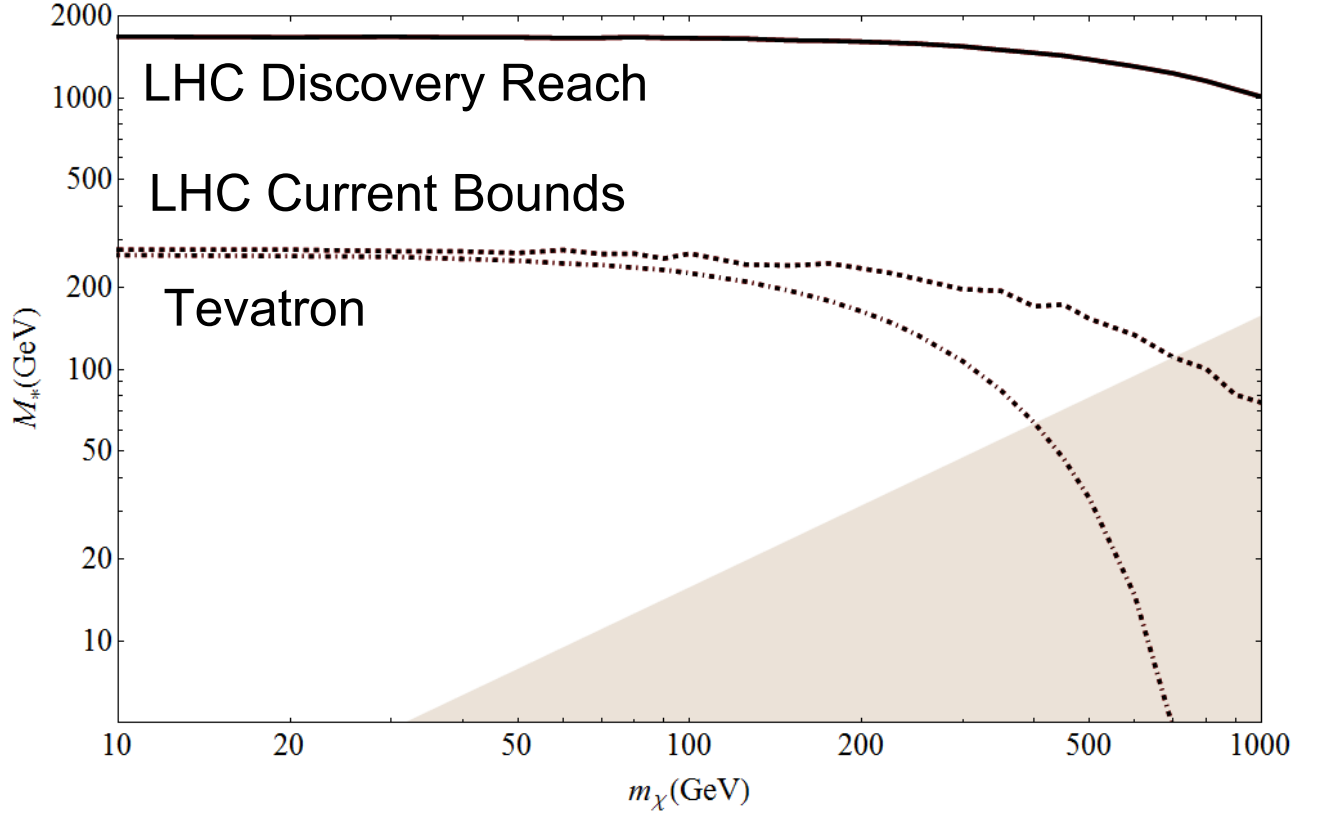


FIG. 4: The same as Fig. 3, although now the up-type quark coupling operators  $M5u$  and  $M6u$  are displayed.

$M_*$ , the resulting cross sections are

$$\sigma^{p,n;SD} = \frac{4\mu_\chi^2}{\pi} \left( \frac{\Delta_u^{p,n}}{M_{*,M6u}^2} + \frac{\Delta_d^{p,n} + \Delta_s^{p,n}}{M_{*,M6d}^2} \right)^2, \quad (6)$$

$$\sigma^{p,n;SI} = \frac{\mu_\chi^2}{\pi} \left( \frac{\sum_u f_u^{p,n}}{M_{*,M1u}^3} + \frac{\sum_d f_d^{p,n}}{M_{*,M1d}^3} \right)^2, \quad (7)$$

where we have adopted the values [49, 50],

$$\begin{aligned} \Delta_u^p &= 0.78, & \Delta_d^p &= -0.48, & \Delta_s^p &= -0.15 \\ f_u^p &= 0.023, & f_d^p &= 0.033, & f_s^p &= 0.05, \\ f_u^n &= 0.018, & f_d^n &= 0.042, & f_s^n &= 0.05, \\ & & f_{c,b,t}^{p,n} &= 0.066, & & \end{aligned} \quad (8)$$

and the neutron and proton spin fractions are related by isospin symmetry.

In constructing models which have particular isospin behavior with respect to protons and neutrons in spin-independent scattering we solve the equation

$$\frac{\lambda_n}{\lambda_p} = \frac{\sum_d f_d^p}{\sum_u f_u^p} \frac{M_{*,M1u}^3}{M_{*,M1d}^3}, \quad (9)$$

where the ratio of neutron to proton couplings is taken as input and we calculate the ratio of suppression scales. The models are then constrained at colliders by noting that there is no interference at leading order between the up- and down-type couplings, which allows us to directly sum the signal cross section from each to find the total cross section expected for a given operator strength.

We translate collider bounds into limits on spin-dependent cross sections in Figures 5–7 for the cases where only the operator M6u is present, the case where only the operator M6d is present, and the case where M6u and M6d have equal couplings. The spin independent bounds are shown on Figures 8-11. The proton scattering cross section bounds for only operators M1u or M1d are plotted in Figure 8 and Figure 9, while Figure 10 shows the bounds assuming both M1u and M1d are present and weighted such that the coupling to the proton and neutron are equal. In Figure 11, we show bounds for  $\lambda_n/\lambda_p = -0.7$ , the central value for isospin violating couplings which reconcile CoGeNT and Xenon.

## V. CONCLUSIONS

We have extended previous studies of collider constraints on dark matter to include isospin-violating effects and updated them to make use of the recent null searches for jets plus missing energy based on  $1 \text{ fb}^{-1}$  of LHC data. Our effective theory description is structured based on MFV to ensure consistency with flavor physics observables and remain as model-independent as possible. In particular, it faithfully reproduces the physics when the particles mediating interactions between dark matter and the SM are significantly heavier than the dark matter particle. We find results which are qualitatively similar to (though quantitatively stronger than) our previous results, with collider limits being the strongest on models of very light dark matter and losing sensitivity as the mass of dark matter approaches the typical energy of collisions at the collider.

Collider constraints on spin-dependent scattering can be appreciably weakened by isospin violation in the UV couplings of dark matter to quarks. Suppressing the coupling to one

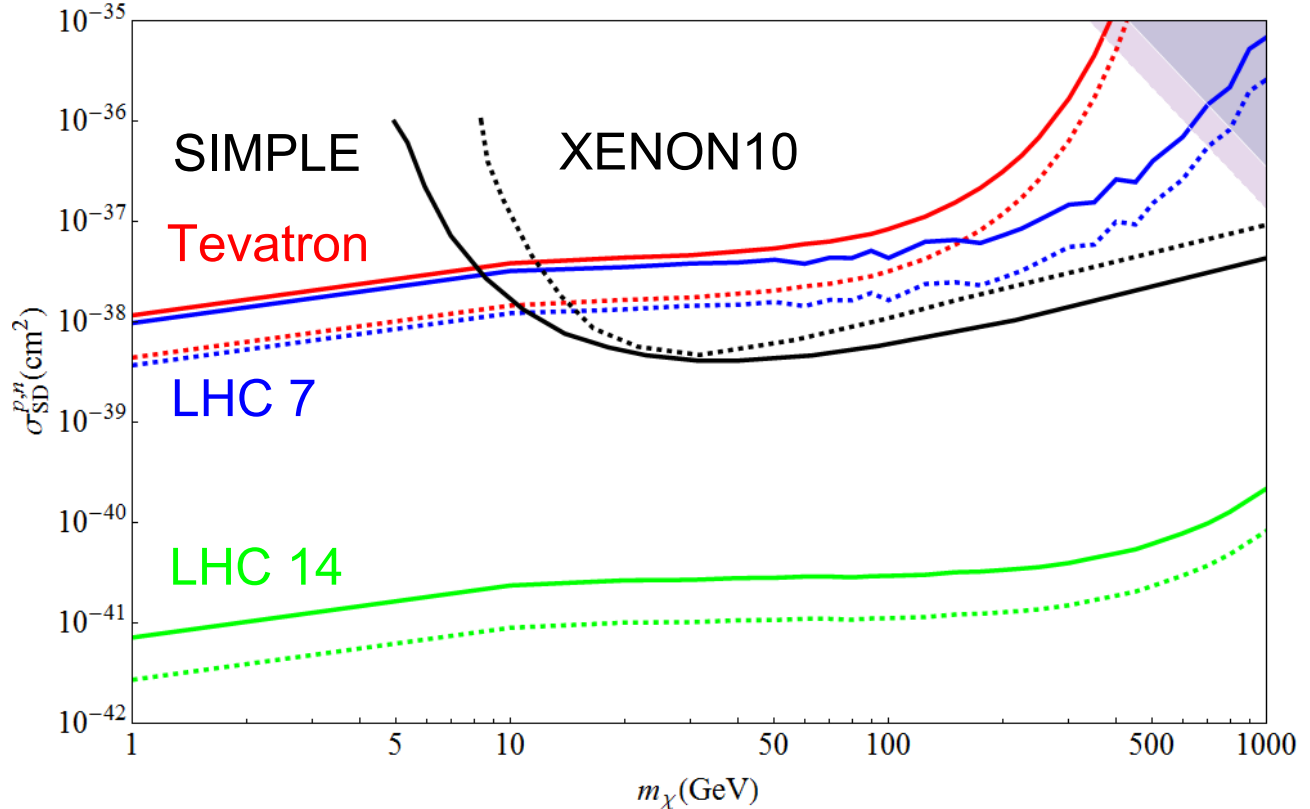


FIG. 5: Spin-dependent nucleon scattering cross section assuming only the up-type quark operator  $M6_u$  is present. The red and blue lines are the constraints from the Tevatron search and 7 TeV LHC search. The green lines are the 14 TeV LHC discovery reach. The solid lines are the proton coupling cross section and the dotted lines are the neutron coupling cross section. The dashed black line is the Xenon 10 constraint on the neutron cross section [51] and the solid black line is the SIMPLE constraint on the proton cross section [52].

type of quarks does not significantly change the production cross section at colliders for dark matter pairs, but it does remove destructive interference in the direct detection scattering cross section, leading to weaker limits from direct detection searches than for isospin conserving cases.

The effects of isospin violation in the spin-independent sector can either strengthen or weaken collider bounds. Suppressing couplings to the heavier down-type quarks significantly decreases the cross section at colliders for mass-suppressed operators, which are the main contributor to spin-independent scattering. However, taking the preferred value for isospin violation which allows CoGeNT to be consistent with Xenon 100 results strengthens collider

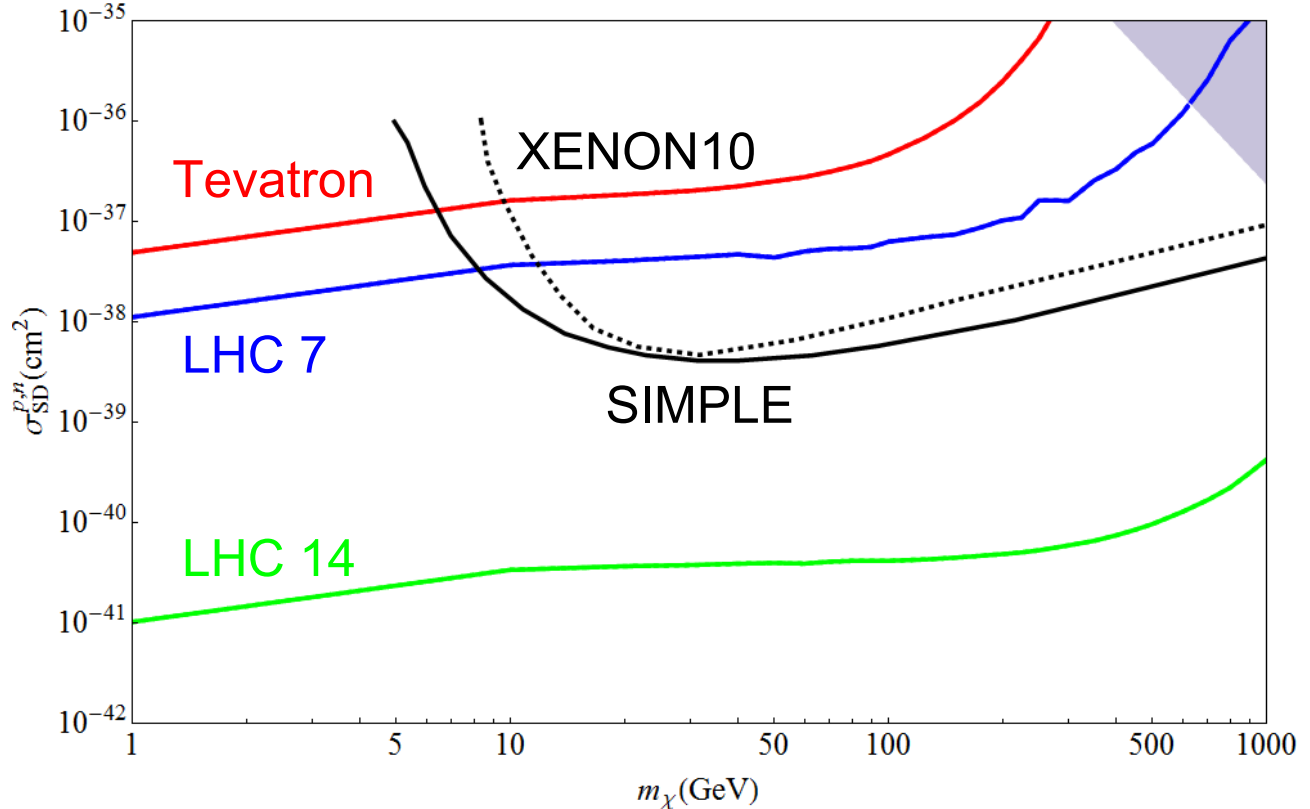


FIG. 6: The same as Fig. 5 but for the down-type quark coupling.

bounds considerably, as it leads to large destructive interference even within a single nucleon as compared to the usual case of isospin conservation. The bounds derived from colliders in this region of parameter space are not only stronger relative to the weakened direct detection experiments, but also stronger in the absolute sense by orders of magnitude. 7 TeV LHC results are already competitive with the strongest direct detection bounds through a large range of dark matter mass in this case, and future LHC reach is better up to masses beyond 1 TeV.

These results are sensitive to the assumption that the particle mediating the dark matter-SM interactions is heavy, and also to the assumption that such interactions obey the MFV hypothesis. In models which predict light mediators or more complicated flavor structures for these interactions those effects need to be taken into account directly, either through using a UV complete description of the dark matter scattering or altering the ratios of couplings between the generations away from the MFV assumptions. Our results indicate that any theory of dark matter which uses the paradigm of isospin violation to reconcile the CoGeNT and Xenon results must either have a collider-accessible mediator responsible

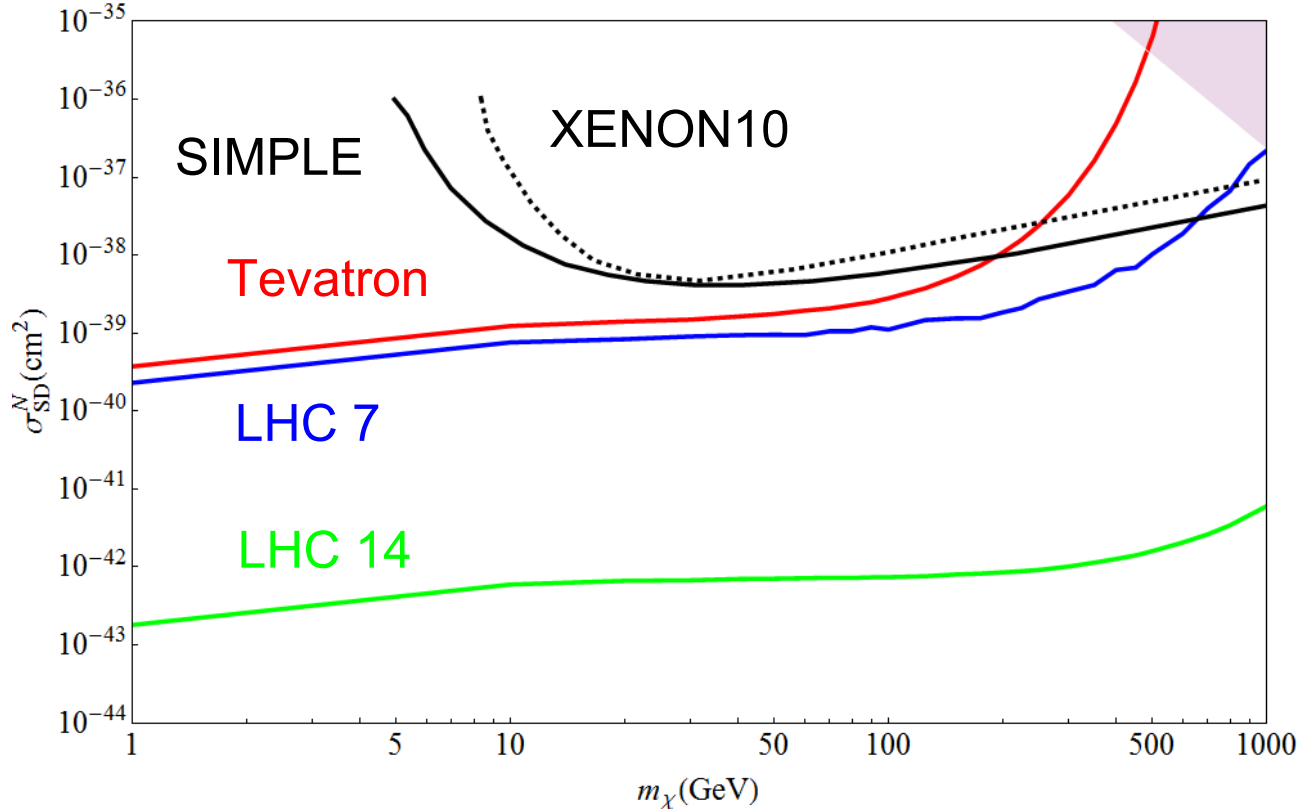


FIG. 7: Spin dependent nucleon coupling cross section assuming equal down and up type couplings. The red and blue lines are the constraints from the Tevatron search and 7 TeV LHC search. The green line is the 14 TeV LHC discovery reach. The dashed black line is the XENON10 constraint on the neutron cross section [51], the solid black line is the SIMPLE constraint on the proton cross section.[52]

for dark matter-SM interactions or have more complicated flavor structure in its couplings. In particular, theories which only couple the dark matter to up and down quarks, and not members of the other generations, are much more difficult to probe at colliders if they interact through mass-suppressed operators.

### Acknowledgements

We thank D. Sanford for helpful conversations. The work of AR is supported in part by NSF grant PHY-0653656. AR would also like to thank the Aspen Center of Physics, where part of this work was completed, for hospitality. The work of TT is supported in part by NSF grant PHY-0970171 and he gratefully acknowledges the hospitality of the SLAC theory

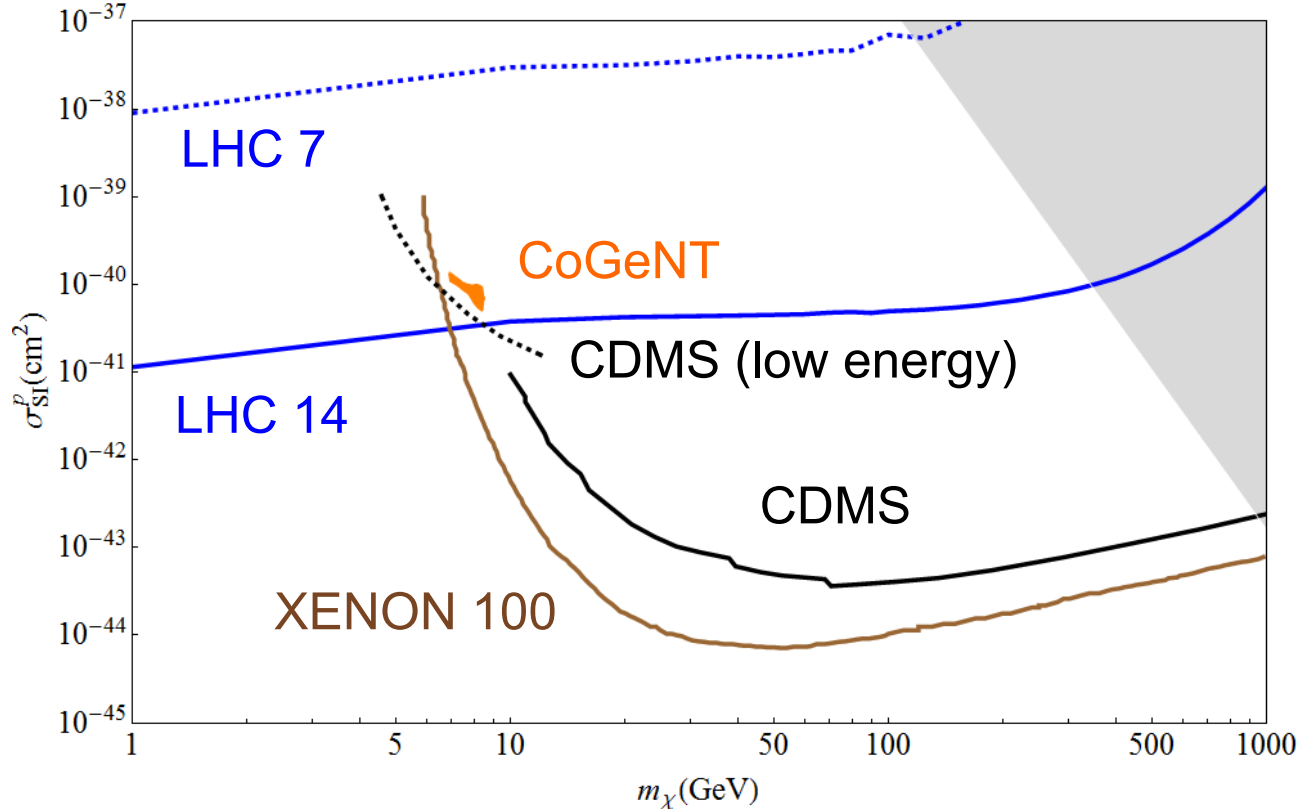


FIG. 8: Spin independent proton scattering cross section assuming only up-type quark coupling. The red line is the constraint from the Tevatron search. The blue lines are the LHC 7 TeV constraint and LHC 14 discovery reach, which are dashed and solid respectively. The brown line is the XENON100 constraint [23]. The black lines (both solid and dashed) are the CDMS constraints [25, 26]. The orange region is CoGeNT favored results.[18]

group, where part of this work was completed. TT and WS acknowledge the hospitality of TASI-2011 at the University of Colorado, where some of this work was undertaken.

- 
- [1] E. Komatsu *et al.*, arXiv:1001.4538 [astro-ph.CO].
  - [2] J. L. Feng and J. Kumar, Phys. Rev. Lett. **101**, 231301 (2008) [arXiv:0803.4196 [hep-ph]].  
J. L. Feng, H. Tu and H. B. Yu, JCAP **0810** (2008) 043 [arXiv:0808.2318 [hep-ph]].
  - [3] A. Birkedal, K. Matchev and M. Perelstein, Phys. Rev. D **70**, 077701 (2004) [arXiv:hep-ph/0403004]; P. Konar, K. Kong, K. T. Matchev and M. Perelstein, New J. Phys. **11**, 105004 (2009) [arXiv:0902.2000 [hep-ph]]; J. L. Feng, S. Su and F. Takayama, Phys. Rev. Lett. **96**,

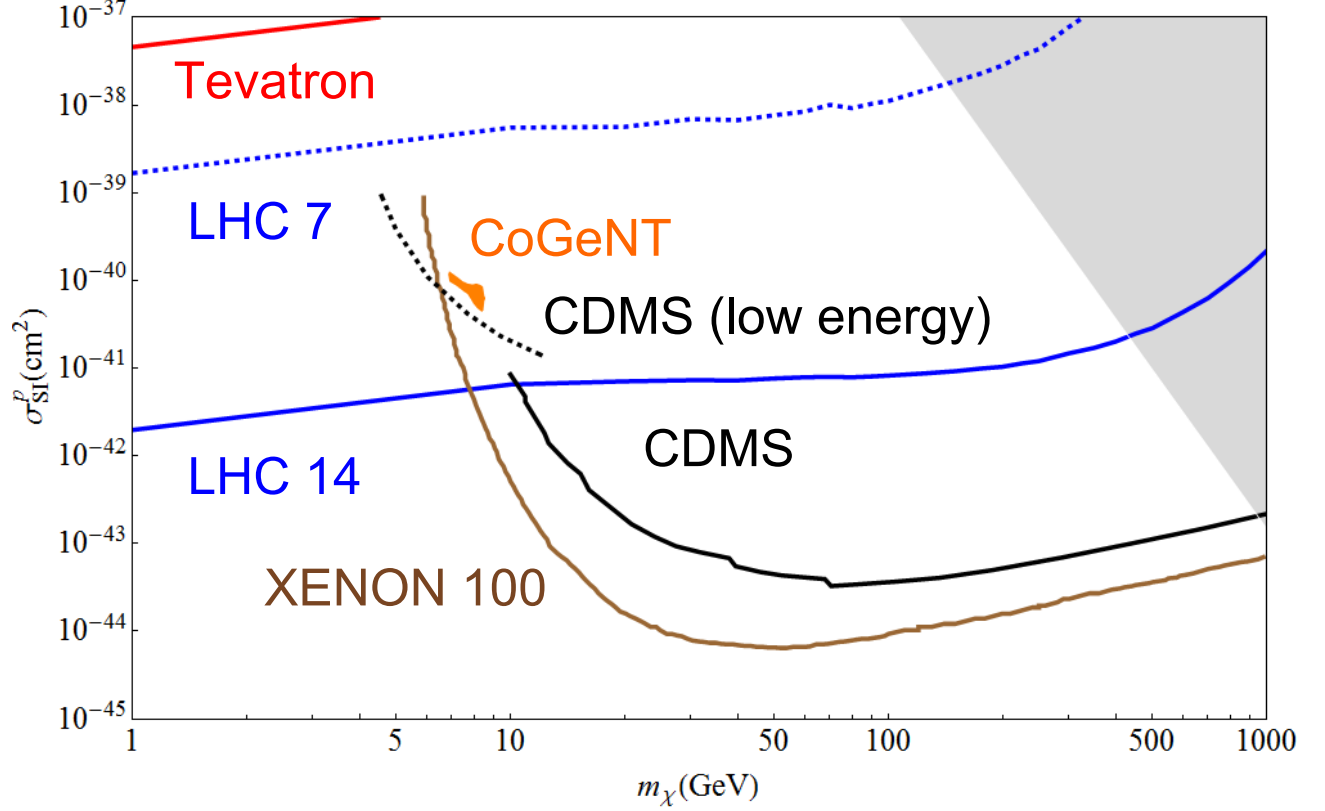


FIG. 9: The same as Fig. 8 but for the down-type coupling.

151802 (2006) [arXiv:hep-ph/0503117].

[4] M. Beltran, D. Hooper, E. W. Kolb and Z. C. Krusberg, Phys. Rev. D **80**, 043509 (2009) [arXiv:0808.3384 [hep-ph]].

[5] Q. H. Cao, C. R. Chen, C. S. Li and H. Zhang, arXiv:0912.4511 [hep-ph].

[6] M. Beltran, D. Hooper, E. W. Kolb, Z. A. C. Krusberg and T. M. P. Tait, arXiv:1002.4137 [hep-ph].

[7] W. Shepherd, T. M. P. Tait and G. Zaharijas, Phys. Rev. D **79**, 055022 (2009) [arXiv:0901.2125 [hep-ph]].

[8] J. Goodman, M. Ibe, A. Rajaraman, W. Shepherd, T. M. P. Tait and H. B. P. Yu, arXiv:1005.1286 [hep-ph];

[9] J. Goodman, M. Ibe, A. Rajaraman, W. Shepherd, T. M. P. Tait, H. -B. Yu, Phys. Rev. **D82**, 116010 (2010). [arXiv:1008.1783 [hep-ph]].

[10] Y. Bai, P. J. Fox and R. Harnik, arXiv:1005.3797 [hep-ph].

[11] P. J. Fox, R. Harnik, J. Kopp, Y. Tsai, [arXiv:1103.0240 [hep-ph]].

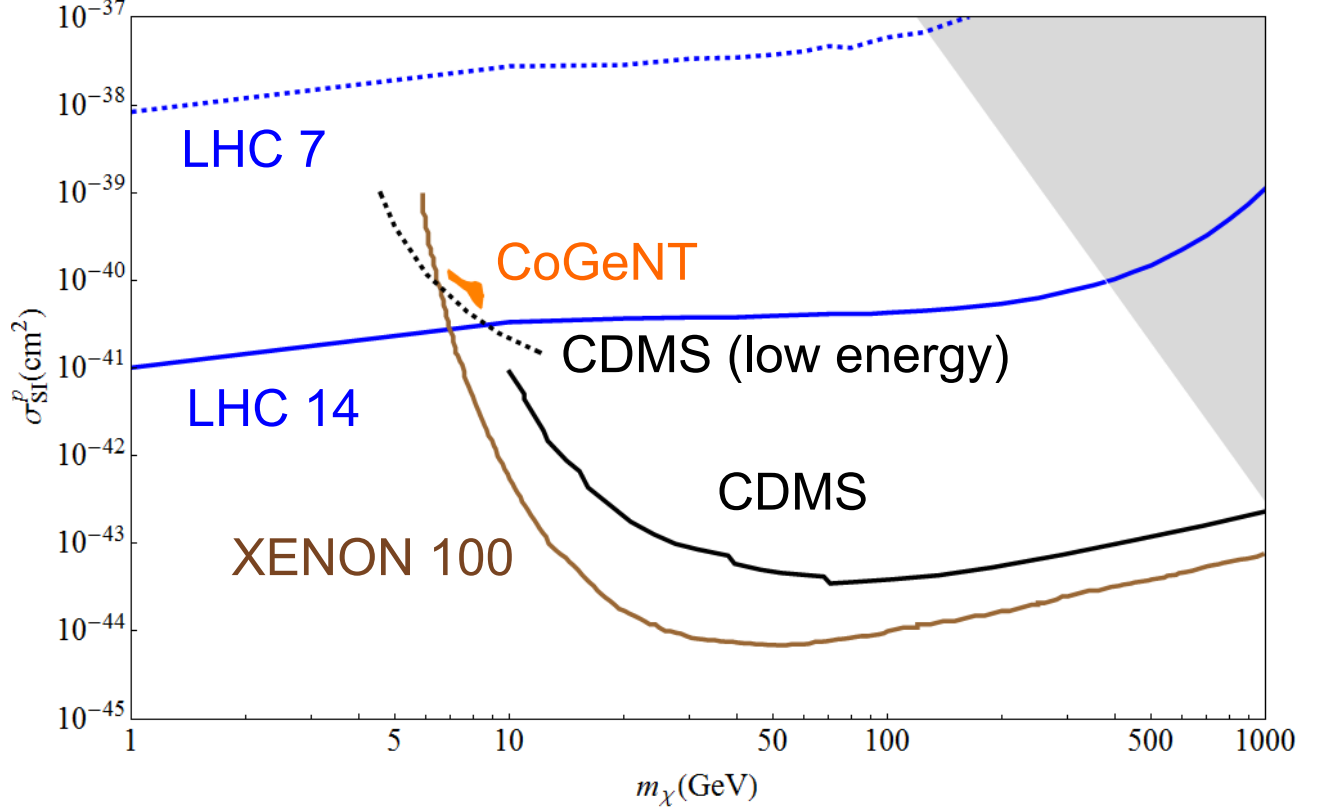


FIG. 10: Spin independent coupling assuming both down and up type couplings such that the proton and neutron coupling is equal. The red line is the constraints from the Tevatron search. The blue lines are the LHC 7 TeV constraint and LHC 14 discovery reach, which are dashed and solid respectively. The brown line is the XENON100 constraint.[23] The black lines (both solid and dashed) are the CDMS constraints.[25, 26] The orange region is CoGeNT favored results.[18]

[12] J. F. Fortin and T. M. P. Tait, arXiv:1103.3289 [hep-ph].

[13] J. F. Kamenik, J. Zupan, [arXiv:1107.0623 [hep-ph]].

[14] C. P. Burgess, M. Pospelov and T. ter Veldhuis, Nucl. Phys. B **619**, 709 (2001) [arXiv:hep-ph/0011335]; H. Davoudiasl, R. Kitano, T. Li and H. Murayama, Phys. Lett. B **609**, 117 (2005) [arXiv:hep-ph/0405097].

[15] S. Kanemura, S. Matsumoto, T. Nabeshima and N. Okada, arXiv:1005.5651 [hep-ph].

[16] K. Cheung, K. Mawatari, E. Senaha, P. Y. Tseng and T. C. Yuan, JHEP **1010**, 081 (2010) [arXiv:1009.0618 [hep-ph]].

[17] J. Wang, C. S. Li, D. Y. Shao and H. Zhang, arXiv:1107.2048 [hep-ph].

[18] C. E. Aalseth *et al.* [CoGeNT collaboration], arXiv:1002.4703 [astro-ph.CO].

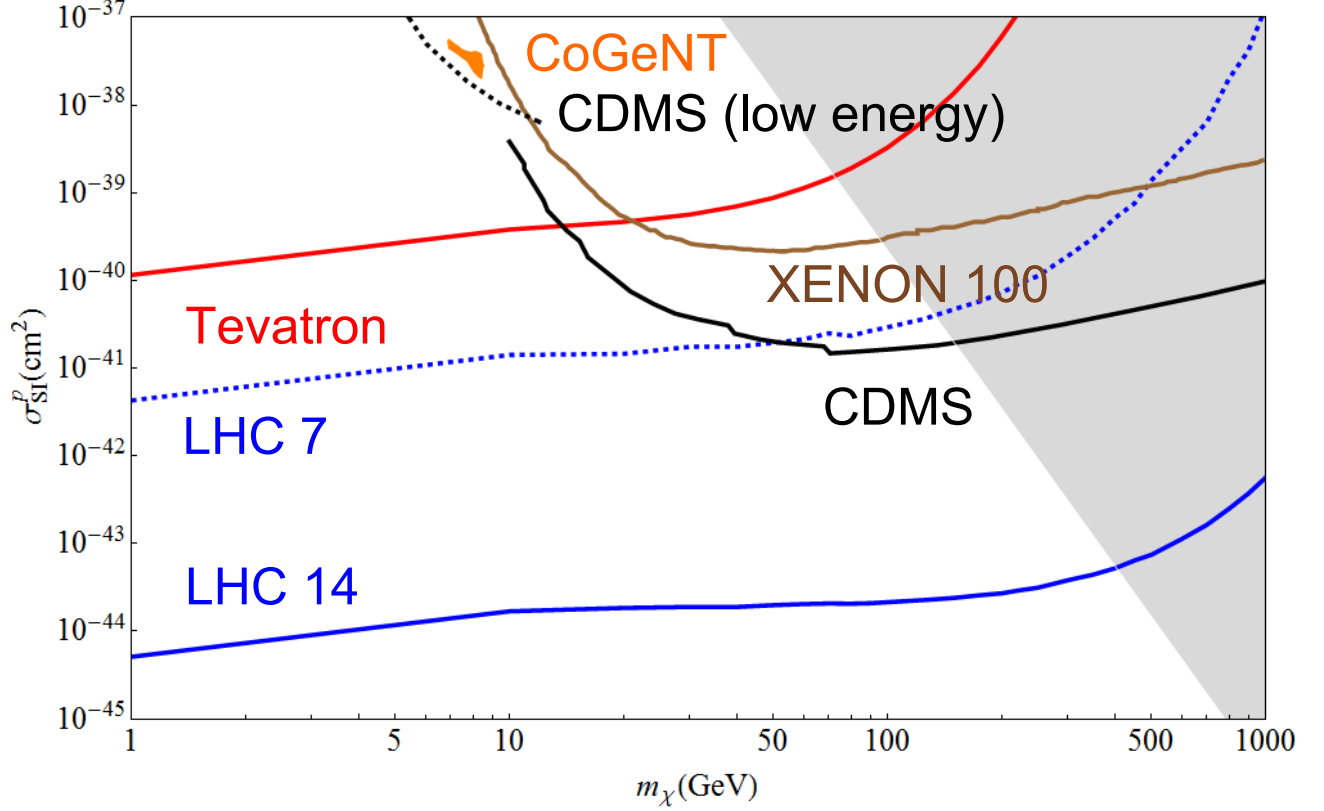


FIG. 11: Spin independent coupling assuming both down and up type coupling such that the neutron to proton coupling ratio is  $-0.7$ . The red line is the constraint from the Tevatron search. The blue lines are the LHC 7 TeV constraint and LHC 14 discovery reach, which are dashed and solid respectively. The green line is the XENON100 constraint.[23] The black lines (both solid and dashed) are the CDMS constraints.[25, 26] The orange region is CoGeNT favored results.[18]

[19] C. E. Aalseth, P. S. Barbeau, J. Colaresi, J. I. Collar, J. D. Leon, J. E. Fast, N. Fields, T. W. Hossbach *et al.*, [arXiv:1106.0650 [astro-ph.CO]].

[20] R. Bernabei *et al.*, arXiv:1002.1028 [astro-ph.GA].

[21] F. Petriello and K. M. Zurek, JHEP **0809**, 047 (2008) [arXiv:0806.3989 [hep-ph]].

[22] J. L. Feng, J. Kumar and L. E. Strigari, Phys. Lett. B **670**, 37 (2008) [arXiv:0806.3746 [hep-ph]].

[23] E. Aprile *et al.* [XENON100 Collaboration], arXiv:1005.0380 [astro-ph.CO].

[24] J. Filippini, “WIMP Hunting with the Cryogenic Dark Matter Search”, Les Rencontres de Physique de la Val le dAosta (2009).

[25] Z. Ahmed *et al.* [The CDMS-II Collaboration], arXiv:0912.3592 [astro-ph.CO].

- [26] Z. Ahmed *et al.* [CDMS-II Collaboration], Phys. Rev. Lett. **106**, 131302 (2011) [arXiv:1011.2482 [astro-ph.CO]].
- [27] T. Schwetz and J. Zupan, arXiv:1106.6241 [hep-ph].
- [28] P. J. Fox, J. Kopp, M. Lisanti and N. Weiner, arXiv:1107.0717 [hep-ph].
- [29] M. Farina, D. Pappadopulo, A. Strumia and T. Volansky, arXiv:1107.0715 [hep-ph].
- [30] J. Fan, M. Reece and L. T. Wang, JCAP **1011**, 042 (2010) [arXiv:1008.1591 [hep-ph]].
- [31] J. Goodman, M. Ibe, A. Rajaraman, W. Shepherd, T. M. P. Tait, H. -B. Yu, Nucl. Phys. **B844**, 55-68 (2011). [arXiv:1009.0008 [hep-ph]].
- [32] K. Cheung, P. Y. Tseng and T. C. Yuan, JCAP **1101**, 004 (2011) [arXiv:1011.2310 [hep-ph]].
- [33] M. R. Buckley, arXiv:1104.1429 [hep-ph].
- [34] A. J. Buras, P. Gambino, M. Gorbahn, S. Jager and L. Silvestrini, Phys. Lett. B **500**, 161 (2001) [arXiv:hep-ph/0007085].
- [35] J. L. Feng, J. Kumar, D. Marfatia, D. Sanford, [arXiv:1102.4331 [hep-ph]].
- [36] S. Chang, J. Liu, A. Pierce, N. Weiner and I. Yavin, arXiv:1004.0697 [hep-ph].
- [37] Z. Kang, J. Li, T. Li, T. Liu, J. Yang, [arXiv:1102.5644 [hep-ph]].
- [38] E. Del Nobile, C. Kouvaris, F. Sannino, [arXiv:1105.5431 [hep-ph]].
- [39] X. Gao, Z. Kang, T. Li, [arXiv:1107.3529 [hep-ph]].
- [40] M. T. Frandsen, F. Kahlhoefer, J. March-Russell, C. McCabe, M. McCullough and K. Schmidt-Hoberg, arXiv:1105.3734 [hep-ph].
- [41] Y. Gao, J. Kumar, D. Marfatia, [arXiv:1108.0518 [hep-ph]].
- [42] J. Alwall, P. Demin, S. de Visscher, R. Frederix, M. Herquet, F. Maltoni, T. Plehn, D. L. Rainwater *et al.*, JHEP **0709**, 028 (2007). [arXiv:0706.2334 [hep-ph]].
- [43] T. Sjostrand, S. Mrenna and P. Z. Skands, JHEP **0605**, 026 (2006) [arXiv:hep-ph/0603175].
- [44] <http://www.physics.ucdavis.edu/~conway/research/software/pgs/pgs4-general.htm>
- [45] T. Aaltonen *et al.* [CDF Collaboration], Phys. Rev. Lett. **101**, 181602 (2008) [arXiv:0807.3132 [hep-ex]].
- [46] <http://www-cdf.fnal.gov/physics/exotic/r2a/20070322.monojet/public/ykk.html>
- [47] The ATLAS collaboration, **ATLAS-CONF-2011-096** (2011).
- [48] L. Vacavant and I. Hinchliffe, J. Phys. G **27**, 1839 (2001).
- [49] G. Bèlanger, F. Boudjema, A. Pukhov, and A. Semenov, Comput.Phys.Commun.180:747-767,2009 [arXiv:0803.2360v2 [hep-ph]]

- [50] J. Giedt, A. W. Thomas and R. D. Young, Phys. Rev. Lett. **103**, 201802 (2009) [arXiv:0907.4177 [hep-ph]].
- [51] J. Angle *et al.* [XENON Collaboration], Phys. Rev. Lett. **100**, 021303 (2008) [arXiv:0706.0039 [astro-ph]].
- [52] M. Felizardo *et al.*, Phys. Rev. Lett. **105**, 211301 (2010) [arXiv:1003.2987 [astro-ph.CO]].